Journal of Environmental Management 293 (2021) 112793

Contents lists available at ScienceDirect

Journal of Environmental Management

journal homepage: www.elsevier.com/locate/jenvman

Household solid waste combustion with wood increases particulate trace metal and lung deposited surface area emissions

H. Timonen [a,*], F. Mylläri [b], P. Simonen [b], M. Aurela [a,b], M. Maasikmets [c], M. Bloss [a], H.-L. Kupri [c,d], K. Vainumäe [c], T. Lepistö [b], L. Salo [b], V. Niemelä [e], S. Seppälä [a], P.I. Jalava [f], E. Teinemaa [c], S. Saarikoski [a], T. Rönkkö [b]

[a] Atmospheric Composition Research, Finnish Meteorological Institute, P.O. Box 503, Helsinki, 00101, Finland
[b] Aerosol Physics Laboratory, Physics Unit, Tampere University, P.O. Box 692, 33014, Tampere, Finland
[c] Air and Climate Department, Estonian Environmental Research Centre, Tallinn, 10617, Estonia
[d] Department of Environmental Engineering, Tallinn University of Technology, Tallinn, 19086, Estonia
[e] Dekati Ltd, Tykkitie 1, Kangasala, Tampere, 36240, Finland
[f] Inhalation Toxicology Laboratory, Department of Environmental and Biological Sciences, University of Eastern Finland, P.O. Box 1627, 70211, Kuopio, Finland

ARTICLE INFO

Keywords:
Biomass burning
Municipal solid waste burning
Particulate emissions
Chemical characterization
Black carbon
LDSA
Metals

ABSTRACT

In households, municipal solid waste (MSW) is often burned along with wood to get rid of waste, to help in ignition or simply to reduce fuel costs. The aim of this study was to characterize the influence of household waste combustion, along with wood, on the physical and chemical properties of particulate emissions in a flue gas of a masonry heater.

The MSW burning alongside wood increased average particulate matter (PM) mass (65%), lung deposited surface areas (LDSA, 15%), black carbon (BC, 65%) concentrations and the average particle size in the flue gas. The influence of MSW was smaller during ignition and burning phases, but especially during fuel additions, the mass, number, and LDSA concentrations increased significantly and their size distributions moved towards larger particles. For wood burning the trace metal emissions were relatively low, but significant increase (3.3–179 -fold increase over cycle) was seen when MSW was burned along the wood. High ratios were observed especially during fuel addition phases but, depending on compounds, also during ignition and burning end phases. The highest ratios were observed for chloride compounds (HCl, KCl, NaCl). The observed increase in light-absorbing particle, trace metal and BC concentrations in flue gas when adding wood with MSW are likely to have negative impacts on air quality, visibility, human health and climate. Furthermore, metals may also affect the condition and lifetime of the burning device due to corrosion.

1. Introduction

As traffic and industrial emissions are continuously decreasing due to stricter emissions regulations, the level of small-scale biomass burning emissions has remained stable and has in many cases steadily increased (e.g. Savolahti et al., 2016, 2019; Helin et al., 2018; Chen et al., 2017). Biomass burning produces a complex mixture of particulate and gaseous emissions (e.g. Chen et al., 2017; Kortelainen et al., 2018) with air quality, health impacts and climate (IPCC, 2013; Janssen et al., 2011; Lelieveld et al., 2015; Timonen et al., 2019). Primary particles are produced during the burning process while secondary aerosol is produced as gaseous emissions partition to the particulate phase due to oxidation of precursor gases during atmospheric processing (Kroll and Seinfeld, 2008; Jimenez et al., 2009). The aerosol between primary and atmospherically aged aerosols is called fresh exhaust or fresh flue gas (Rönkkö et al., 2017). In fresh exhaust aerosol, the exhaust/flue gas has cooled to ambient temperatures and a significant part of semi volatile exhaust compounds have condensed or nucleated into the particulate phase. Many studies have investigated primary and fresh particulate emissions and their influence to urban air quality by direct sampling from the hot emission gases in the biomass burning plumes (e.g. Tissari et al., 2008; Cubison et al., 2011; Hennigan et al., 2011; Maasikmets et al., 2016). Primary and fresh particulate emissions from biomass burning mostly consist of carbonaceous matter (organic and black

* Corresponding author. P.O.Box 503, 00101, Helsinki, Finland.
E-mail address: hilkka.timonen@fmi.fi (H. Timonen).

https://doi.org/10.1016/j.jenvman.2021.112793
Received 14 December 2020; Received in revised form 28 April 2021; Accepted 13 May 2021
Available online 28 May 2021

carbon), as well as some inorganic ions (chloride, sulphate) and metals (e.g. K, Na, Zn, Fe) (Kortelainen et al., 2018; Chandrasekaran et al., 2012). Secondary PM formation from gaseous precursors originating from biomass burning can be studied using oxidation flow reactors (OFR) (e.g. Kang et al., 2007; Lambe et al., 2015; Simonen et al., 2017; Ihalainen et al., 2019). Results from previous studies have revealed a great range, varying from a high level of SOA production to very little or no SOA production, in the generation of secondary organic aerosol (SOA) from biomass burning (e.g. Cubison et al., 2011; DeCarlo et al., 2010; Ortega et al., 2015).

It is estimated that globally 1 to 2 billion metric tons of municipal solid waste (MSW), i.e., household wastes such as organic waste, cardboard and plastic packaging as well as waste from industrial, institutional and commercial sources, are produced yearly (Wiedinmyer et al., 2014). Although the small-scale waste burning in households is mostly banned, still a large percentage of households (e.g. in Finland >40%, (Ohtonen et al., 2018), in Estonia >30% irregularly and around 2% regularly (Maasikmets, 2019)) burn waste, such as cardboard, newspapers, cartons etc, along wood. In households, MSW is often burned along with wood to get rid of waste, to help in ignition or simply to reduce fuel costs. In developing countries, with poor waste disposal systems, MSW may also be burned in open, uncontrolled fires (Meallem et al., 2010; Stockwell et al., 2016; Rivellini et al., 2017; Jayarathne et al., 2018). Residential waste burning can significantly contribute to air pollutant concentrations near emission sources but also to the air quality of larger areas. For instance, in urban air, organic aerosol originated from plastic burning has been found during cold season in Estonia (Maasikmets et al., 2015). In the study of Argyropoulos et al. (2012), waste burning was contributing on average 7.8–14.3% (cold season) and 3.3–10.2% (warm season) to the ambient PM_{10} at two studied sites located in the Rhodes Island, Greece.

The combustion of wood in households causes adverse effects for human health and even mortality and morbidity (e.g. Forouzanfar et al., 2015; Muala et al., 2015; Lim et al., 2010). The toxicity of combustion aerosol depends on various factors related e.g. to combustion condition, fuel quality, particle composition (e.g. Jalava et al., 2012; Kasurinen et al., 2016). The release of potentially toxic compounds, e.g. polycyclic aromatic hydrocarbons (PAHs) has been observed to increase, depending on the waste type (Jayarathne et al., 2018; Hoffer et al., 2020). Wagner and Cabarello (1997) studied the combustion of rubber and plastic-type materials and found highly toxic gases such as hydrocyanic acid, sulphur dioxide, and hydrogen chloride in emitted compounds. In their study, more than 92% of the particulate mass was found to be in the respirable range, and toxic heavy metals such as lead, chromium, and antimony emissions were also detected in particles. Also, Hedman et al. (2006) identified a variety of different toxic compounds, including e.g. polychlorinated dibenzodioxins/dibenzofurans (PCDD/F's) in emitted smoke for the combustion of MSW in stoves. These toxic compounds from waste burning may cause health risks if humans are exposed to the emitted compounds (e.g. Menezes-Filho et al., 2012; Gangwar et al., 2019).

The aim of this study was to characterize the influence of household waste combustion along with wood on the physical and chemical properties of particulate emissions. A masonry heater was used to burn the wood and MSW and a comprehensive set of instruments was used to measure physical and chemical properties of particles, including detailed chemical composition, number- and mass concentrations, as well as lung deposited surface areas (LDSA), number and mass size distributions of PM, during the burning process in the flue gas.

2. Experimental

2.1. Measurement and dilution setup

The experiments were conducted at the Estonian Environmental Research Centre (EERC) fireplace test facility in Tallinn, Estonia. The fireplace was a masonry heater constructed to closely resemble fireplace built according to the standard EN 15544. The measurement setup is shown in Fig. 1. The flue gas sample was taken from the back of the heater from the base of the chimney, i.e., relatively close to the combustion process. The flue gas sample was first diluted using an ejector (Dekati Ltd, Finland) diluter, followed by pair of secondary diluters. A set of instruments measuring gaseous and particulate emission were placed after the other double ejector system. In addition, another ejector diluter after the PAM was used to dilute the flue gas sample further to concentrations suitable for the aerosol instruments. The average dilution ratio was 108 after the double ejectors and 2099 after the PAM (i.e. last ejector dilutor). A detailed description of dilution setup and dilution ration calculations is given in Supplemental material. The CO concentration of the sample was measured before the PAM chamber with a Fourier transform infra-red analyzer (FTIR, Gasmet) and after the PAM with Environnement S.A, CO12M analyzer). The CO concentrations were used to calculate the OH-exposure of the sample.

Two Electrical Low-Pressure Impactor (ELPI) units were used in this study: a classic ELPI (cELPI; Keskinen et al., 1992; Marjamäki et al., 2000) and ELPI+ (Järvinen et al., 2014). Both devices share the same operating principle. Shortly, ELPI devices charge the measured particles in a diffusion charger and then classify the particles according to their aerodynamic size in a cascade impactor. The electrical current imparted by the collected particles in the impactor stages are measured with 1 s time resolution. The current data can then be converted to various particle size distributions. In this study, ELPI+ was used to determine particle number size distribution, mass size distribution and LDSA size distribution. The LDSA size distribution was calculated by using stage-specific conversion factors presented in Lepistö et al. (2020). The cELPI unit was used to monitor particle mass concentration after the PAM chamber. The cELPI was modified with an additional stage (Yli-Ojanperä et al., 2010) and a filter-stage (Marjamäki et al., 2002) to nearly resemble the ELPI + impactor configuration. Data from impactor stages that received less than 0.5% of the total current after secondary collection corrections were ignored. A previous article from this campaign compared instruments for particle mass measurements (Salo et al., 2019).

A Soot-particle Aerosol Mass Spectrometer (SP-AMS, Aerodyne Research Inc, US) was used to gain information on the real time chemical composition of submicron non-refractory PM (sulphate, ammonium, nitrate, chloride, organics), refractory organics and refractory BC (rBC) and some metals (Onasch et al., 2012; Carbone et al., 2015). The SP-AMS contains a standard tungsten vaporiser and a Nd:YAG laser vaporiser (1064 mm), which allows the SP-AMS to measure refractory PM that

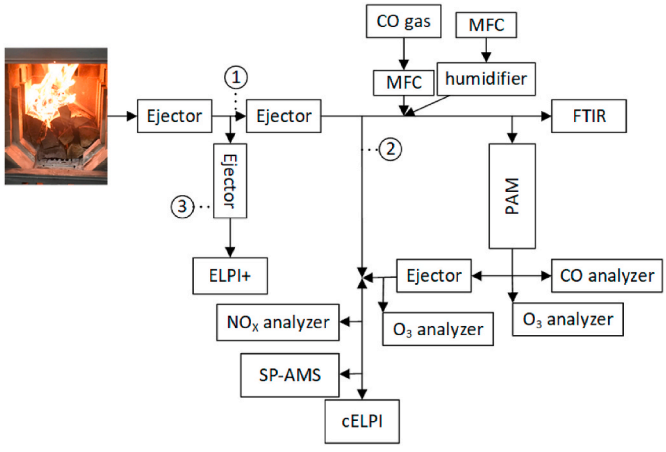

Fig. 1. Experimental setup used to measure wood and MSW burning emissions. Numbers 1–3 represent the locations of CO_2 measurements for dilution ratio calculations. Mass flow controllers (MFC) were used to control the CO and humidifier flows.

vaporises above the tungsten vaporiser temperature (600 °C). The measured particle size range of the SP-AMS is limited by the aerodynamic lens, which transmission efficiency is over 50% for particles with vacuum aerodynamic diameter between approximately 50-700 nm (Liu et al., 2007).

The SP-AMS data was analysed using AMS software (SQUIRREL 1.60 and PIKA v1.20) with Igor Pro 6.37 (WaveMetrics, OR). Collection efficiency (CE), calculated based on the Middlebrook et al. (2012), was between 0.5 and 1. In general, CE was 0.5, which was therefore used for all data points. A CO_2 correction for the SP-AMS data was done as there was relatively large variation in CO_2 concentration.

A Potential Aerosol Mass (PAM) chamber (Aerodyne Research Inc, US, Kang et al., 2007; Kang et al., 2011) was used to simulate the atmospheric aging of the flue gas. The PAM chamber is a small flow through chamber with two UV lamps to produce UV radiation ($\lambda = 185$, 254) and high oxidant (O_3, OH and HO_2) concentrations (100–1000 times tropospheric values). The ratios of OH/O_3 and HO_2/OH are similar to tropospheric values and the PAM chamber is shown to simulate well atmospheric conditions (Kang et al., 2007; Lambe et al., 2011, 2015). The flow through the PAM chamber was 9 L min^{-1}, which was divided to central flow (7.5 L min^{-1}) and ring flow (1.5 L min^{-1}). The latter one was used to reduce interactions with the walls, and it was discarded. At the flow rate of 9 L min^{-1}, the calculated average residence time in the PAM chamber was 88 s. The set voltage of the PAM chamber lamps was 2.5 V, the average temperature and relative humidity (RH) were 25.8 ± 1.7 °C and 24.2 ± 1.4%, respectively. The loss and OH-exposure calculations described in supplemental material.

2.2. Burning experiments

During the measurement campaign a total of five burning experiments were conducted (Table 1). Each burning experiment typically lasted for 60–90 min. The fireplace was allowed to cool between each experiment for at least an hour and for the cooling blower at the top of the chimney was used. The burned material was either pure dry wood (alder and spruce, less than 20% humidity) or wood with added MSW (Table 1). MSW was present at the ignition and it was added simultaneously with wood during the additions. The MSW consisted of a typical household waste, excluding any chemical/paint/glue containers (Table 2). The percentages of each waste fraction were based on the Estonian municipal solid waste sorting study (SEI, 2013). Waste materials were not shredded before the combustion and were packed into a light-weight plastic bag to ensure that every bag had a similar variety of materials to represent each material group chosen for the experiments from the MSW sorting study.

Burning conditions were categorized to four phases called: ignition, burning, addition and end burning. The ignition phase began by lighting kindling (small sticks of the wood) placed on top of the logs. The chosen 'top down' ignition method was used as it should prevent the smouldering at the beginning of the experiment. The ignition was made with 5–8 kg batches of dry wood logs (Table 1), which were dried in a room temperature conditions and weighted before use. In experiments 4–5 the wood was ignited with MSW.

Table 1
Amount of fuel (kg) used in burning experiments, shown separately for ignition and subsequent additions. Fuel additions not characterized due to the technical difficulties during experiments are marked with *.

Fuel	Wood	Wood	Wood	Wood + MSW	Wood + MSW
Cycle no.	1	2	3	4	5
Wood in ignition (kg)	5.15	7.92	6.28	5.63 + MSW	5.05 + MSW
1. Addition (kg)	2.07*	4.18	3.02	2.17*	3.89 + MSW
2. Addition (kg)	2.23*	3.84	2.65	4.0 + MSW	3.12 + MSW
3. Addition (kg)	1.44	–	–	5.01 + MSW	–
4. Addition (kg)	2.2	–	–	–	–
Total mass (wood, kg)	13.09	15.94	11.95	16.78	12.06

Table 2
MSW material types, weight (g) and contribution (%) of each material used in the cycles 4 and 5.

Material	Amount of MSW, experiment 4 (g)	% of MSW	Amount of MSW, experiment 5 (g)	% of MSW
Plastic	257	31.5	259	32.8
Paper and cardboard	194	23.8	193	24.5
Wood	28.7	3.5	28.8	3.6
Other flammable material	263	32.2	235	29.7
Textile	72.6	8.9	73.8	9.3
Total mass	**816**	**100**	**790**	**100**

Burning phase was the phase after ignition when most of the fuel was in visible flames and the temperature in the fireplace had increased. The burning phase is the optimum operating condition for the masonry heater with a high temperature and adequate oxygen feed to the combustion. During burning phase, temperatures reached in combustion chamber an average of 425 °C and occasionally a peak temperatures up to 649 °C were observed. Next batch of fuel was added after most of the previous fuel had burned until embers. Third phase of the experiment was the addition of the fuel. The stage from last addition to end of experiment was called end burning. The fireplace was allowed to cool between each experiment for at least an hour. A blower situated at the top of the chimney was used to keep the gas velocity constant (~2 m s^{-1}) and to aid the cooling of the masonry heater. At the beginning of each experiment, temperature at the masonry heater was between 20 and 130 °C, depending on the cycle. The effect of fireplace's temperature, at the beginning of cycle, was estimated to have minor influence on flue gas emissions. Tables S1 and S2 contains a summary of measurement points, used fuels and different burning conditions as well as average gaseous and particulate emissions during different phases.

The gaseous emissions, CO, NO_x, were relatively similar between all cycles (NO_x 0.63–0.97 g/kgCO_2, CO 11.3–18.6 g/kgCO_2) and no major changes in emission levels were observed due to addition of MSW. The temperature of the combustion was relatively low and, thus the NO_x emissions are most probably originated from the fuel. The highest CO emission factors were measured in the burning end phase for both wood and wood + MSW combustion. Average modified combustion efficiencies (MCE's, table S1) were similar for all cycles (0.97–0.98) for the flaming-dominated burning (Pokhrel et al., 2021), however the MCE's were between 0.92 and 0.93 in the burning end phase of wood + MSW combustion but between 0.93 and 0.95 in the burning end phase of wood combustion.

We note that the fireplace used in the study is a fireplace commonly used in the Nordic households and wood burning is a common practice. Waste mixture was chosen to represent commonly burned trash. Thus, the results are generalizable to freshly emitted household combustion emission, but, however, not to waste burning plants or open fires in ambient conditions and waste dumping sites. We note that the combusted waste, and combustion conditions may have a large influence on emissions. Also, in the atmosphere emitted flue gas is diluted, cooled, mixed with ambient pollution and transformed during the aging process. Our results represent both fresh emissions and secondary aerosol formation potential of emissions during aging.

3. Results and discussion

3.1. Influence of MSW to observed number size distribution

Altogether five burning experiments to characterize gaseous and

particulate emissions were conducted. In three experiments, the fuel was wood (cycles 1–3) and in two experiments fuel was a mixture of wood and municipal solid waste (wood + MSW, cycles 4–5). To study the temporal behaviour of emissions and the influence of MSW on particle number (PN) concentrations and size distributions, two of the cycles (cycle 3 wood as fuel and cycle 5 wood + MSW) were chosen for more detailed timeseries analysis as they had continuous fresh PN measurements during the whole cycle.

Fig. 2 shows the particle number size distribution in fresh flue gas as a function of time for wood (upper panel) and wood and MSW burning (lower panel). Timeseries for other cycles are shown in supplemental material (Fig. S1-3). In all cycles, the ignition of the fuel produced a burst of small particles with particle diameters between 10 and 100 nm. After approximately 5 min from the beginning, i.e., when the fuel started to burn efficiently, a relatively stable particle mode between aerodynamic diameters of 80 and 300 nm and with mean particle size around 150 nm was observed. During the fuel additions, high concentrations of small particles with diameters 10–100 nm appeared again in the particle number size distribution. However, this phenomenon was short lasting, and more significant change in the particle size distributions was seen in larger particles; the addition of fuel significantly increased their concentrations for 3–5 min, mostly in particle sizes larger than 80 nm. Note that during the fuel additions, the upper part of the particle number size distributions clearly reached even micrometer size. At the end of the burning cycles, the mean particle size decreased gradually, and concentrations decreased in all particle sizes. Similar particle size distributions from wood combustion, in the size range100-200nm (the mode with the highest concentration) has been reported by Tiwari et al. (2014). Kortelainen et al. (2015) measured the geometric mean diameter of particles from wood combustion varying between 40 and 150 depending on the burning phase and wood species. Hosseini et al. (2010) reported smaller particle sizes from the combustion of different wood types in laboratory conditions with the mode at around 30–50 nm for mixed state combustion (small flames and smouldering) and concentrations decreasing sharply after 200 nm. Similarly, to this study number, surface area and mass concentrations peaked at ignition and after new patch addition in measurements by Kortelainen et al. (2015) and Hosseini et al. (2010) also reported a significant reduction of particle number concentrations as burning proceeded.

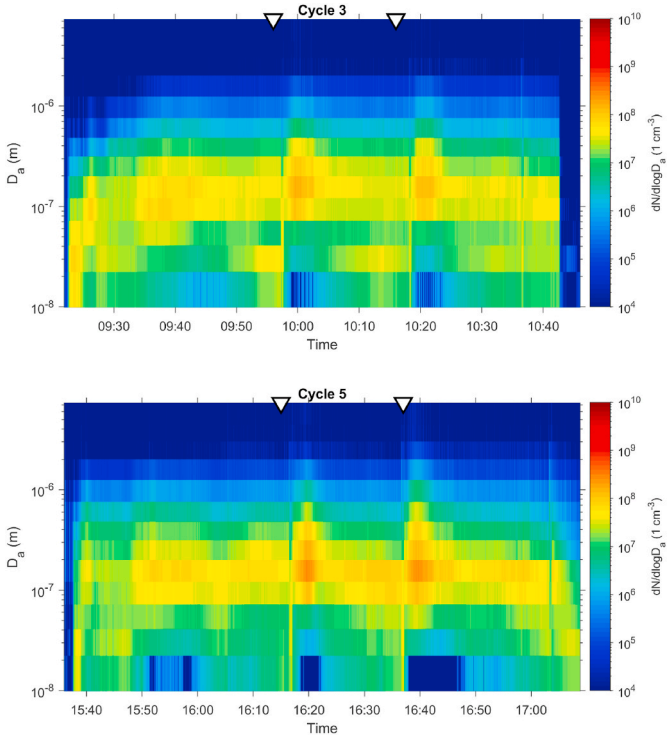

Fig. 2. Fresh flue gas particle number size distributions as a function of time for wood burning (cycle 3, upper panel) and wood + MSW burning (cycle 5, lower panel). PN measurements were conducted with the ELPI + after the double ejector dilution of flue gas. Cycle 3: ignition 09:21–09:38, burning phase 09:44–09:49, fuel additions at 9:56 and 10:16 and burning end 10:27–10:46. Cycle 5: ignition 15:36–15:49, burning phases 15:50–16:05 and 16:07–16:15, fuel additions at 16:15 and 16:37 and burning end 16:49–17:08.

Although the temporal behaviour for both fuels were similar, fuel clearly affected the observed PN concentration levels. In the wood burning, the mean PN concentration, corrected by dilution ratios, was approximately 4.2×10^7 cm^{-3} and in the combination of wood and MSW burning it was 12% higher (4.7×10^7 cm^{-3}) (Table 3). Increase of particulate emissions due to the burning of MSW with wood can be also observed from measured flue gas mean PM_1 and $PM_{2.5}$ particle mass (81–100% increase) and LDSA (56% increase) concentrations (Table 3). In general, particle number and mass concentration levels for wood combustion were relatively similar as observed in previous studies (e.g. Kortelainen et al., 2018). Previous studies have shown that both the fuel and combustion conditions has significant impact on emissions (Tissari et al., 2008; Kortelainen et al., 2018). Likely in this study the change in fuel from wood to wood + MSW, changed both the fuel and the combustion conditions and thus caused increase in emission levels. Inline with our results, Hoffer et al. (2020) observed 1 to 38 times higher PM_{10} emission for waste combustion, depending on burned waste, when compared to wood combustion. Also, Jayarathne et al. (2018) observed significantly higher $PM_{2.5}$ emission factor for damp garbage than dry garbage (dry garbage $EF_{PM2.5}$ 7.4 g/kg, damp garbage $EF_{PM2.5}$ 125 g/kg).

3.2. Influence of MSW to LDSA size distributions

Fig. 3 and supplement Figs. S4-7 show the LDSA size distributions for the wood and wood + MSW burning in different phases (ignition, burning, addition, burning end) of cycle 5 (Fig. 3) and cycles 1–4 (Fig S4-7). Table S3 summarizes the average LDSA concentrations calculated per kg (CO_2) and geometric mean particle sizes (D_a) of LDSA size distributions for different cycle phases. In general, the CO_2 normalized LDSA concentrations were slightly lower ($2.4–5.4 \times 10^{12}$ μm^2/kg$_{CO2}$) for wood burning than for wood and MSW burning ($2.2–6.4 \times 10^{12}$ μm^2/kg$_{CO2}$). The mean D_a for wood combustion was 0.19 μm (cycles 1–3) and 0.24 μm for wood + MSW combustion (cycles 4–5). The lowest particle sizes were seen during wood ignition (0.11-0-13 μm) and end burning (0.17–0.19 μm). In contrast, the largest mean aerodynamic particle sizes were seen during wood and MSW additions (0.26–0.31 μm). As the largest change in emissions for both PN and LDSA was observed during fuel additions, these periods were chosen for further examination (chapter 3.3.).

Although, the recent scientific literature reports LDSA concentrations and emission factors e.g. for traffic and ambient air (e.g. Kuuluvainen et al., 2016; Järvinen et al., 2019; Cheristanidis et al., 2020), information about LDSA concentrations and size distributions from wood or Wood + MSW combustion are scarce. Kortelainen et al. (2018) published average surface area concentrations measured with NSAM (Nanoparticle Surface Area Monitor) for birch combustion (1.6×10^6 μm^2 cm^{-3}) and for spruce combustion (8.7×10^5 μm^2 cm^{-3}). Similarly,

Table 3
Mean PN, LDSA, PM_1 and $PM_{2.5}$ concentrations for wood (cycles 3) and wood + MSW (cycle 5) burning cycles.

Cycle	3	5
Mean PN	4.2×10^7 cm^{-3}	4.7×10^7 cm^{-3}
Mean LDSA	2.3×10^5 μm^{2}cm^{-3}	3.6×10^5 μm^{2}cm^{-3}
Mean PM_1	1.1×10^5 μg m^{-3}	2.0×10^5 μg m^{-3}
Mean $PM_{2.5}$	1.2×10^5 μg m^{-3}	2.4×10^5 μg m^{-3}

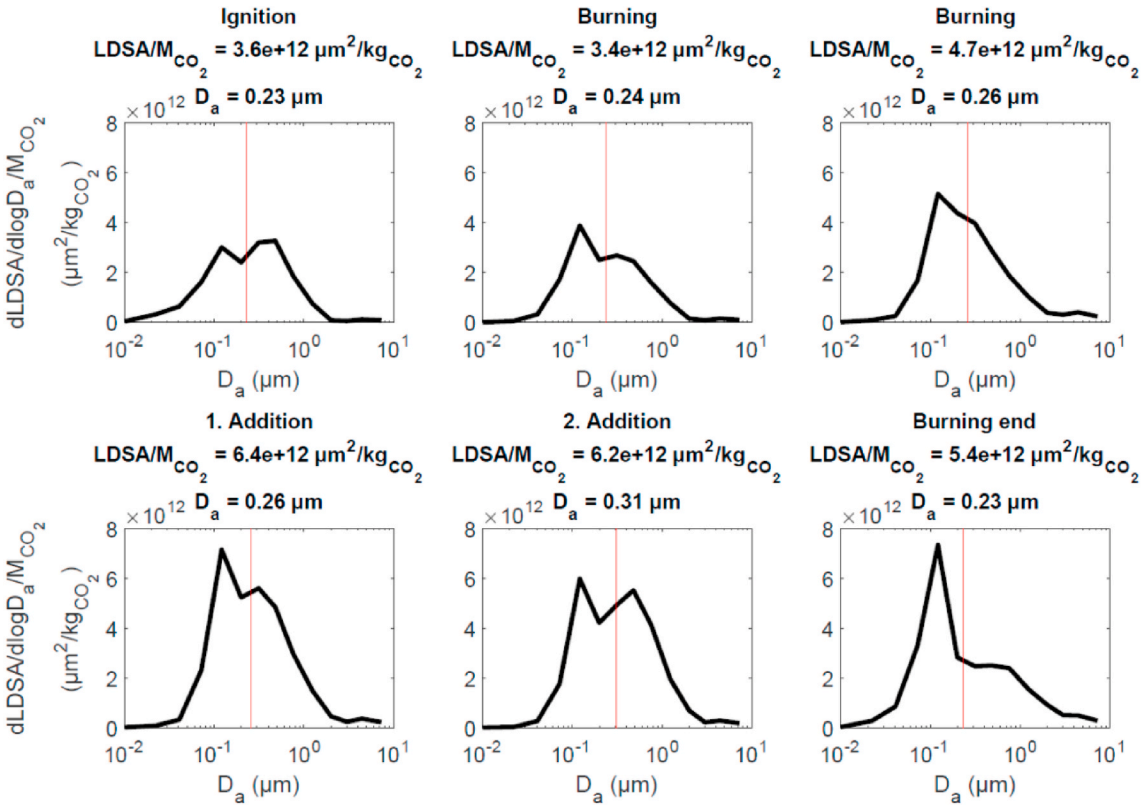

Fig. 3. LDSA size distributions for different phases of wood + MSW burning cycle (cycle 5). The phase of the burning mentioned in subfigure titles together with normalized LDSA concentrations and mean LDSA size (indicated also by red vertical line). Results of other cycles 1–4 shown in supplementary material Figs. S4-7. (For interpretation of the references to color in this figure legend, the reader is referred to the Web version of this article.)

to our study, they observed highest surface area concentrations during the batch additions. It has been previously seen that changes in LDSA concentration may affect to various health parameters, e.g. lung function (Patel et al., 2018).

3.3. *Influence of MSW to flue gas particle size distributions during fuel additions*

Fig. 4 shows the particle size distributions for number, LDSA and mass concentrations of the fresh aerosol during the Wood and Wood + MSW addition phases. The results of other measured additions are shown in Fig. S8.

The observed number, LDSA, and mass concentrations in all the size distributions were significantly higher in the wood + MSW addition (dashed line) when compared to wood addition. Differences were seen also in particle sizes; the geometric mean particle diameters were 109 nm for the number size distribution, 261 nm for the LDSA size distribution and 491 nm for the mass size distribution during the first addition of wood + MSW and, respectively, in the first addition of wood those were 84 nm (number), 223 nm (LDSA) and 408 nm (mass). This behaviour was repeatable which can be seen as highly similar size distributions during the second fuel addition (Fig. 3b).

All particle size distributions presented in Fig. 4 covered large particle size range. Regarding particle number, the highest concentrations were in approximately 100 nm, but the tail of the distribution continued down to 10 nm and, on the other hand, up to 500 nm. MSW additions increased the observed particle number concentrations but it did not affect much the shape of the number size distributions. The LDSA size distributions covered the whole fine particle size range, i.e., particle sizes smaller than 2.5 µm. It is important to notice that the MSW caused

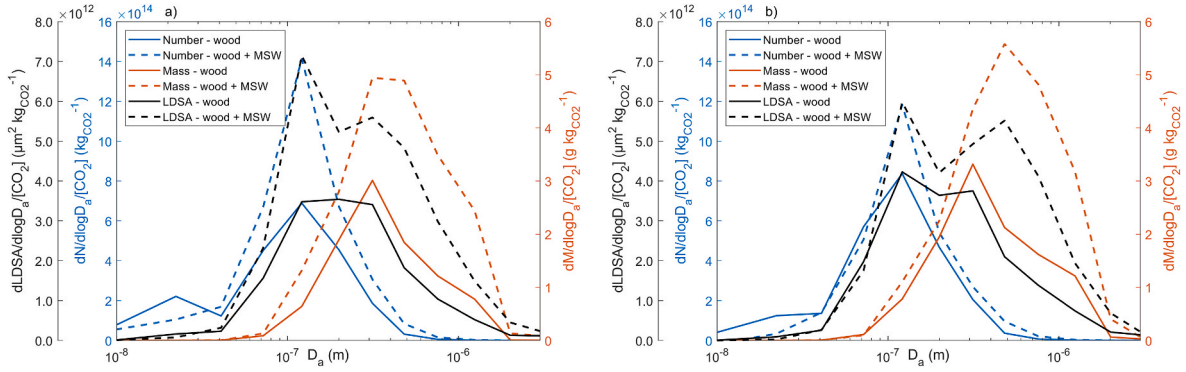

Fig. 4. The mean particle size distributions for number, LDSA and mass for fresh aerosol during the first (a) and the second (b) addition of wood or wood + MSW. The size distributions have been normalized with CO_2 emissions (kg_{CO2}). Data are from experiments 3 (wood) and 5 (wood + MSW).

a significant change also for the shape of LDSA size distribution; while the LDSA size distribution was nearly one-modal in case of wood additions, during wood + MSW additions it was clearly bimodal. The second mode appeared in 200–1000 nm particle sizes. This was seen also in the mean particle sizes of LDSA mentioned above (Table S3). The measured particle mass size distributions covered sizes from 100 nm to the sizes significantly above 1 μm. The particle mass size distributions related to wood burning had nearly one-modal shape, with relatively weak "shoulder" in sizes above 1 μm. In case of MSW addition, this "shoulder" increased and formed a major part of the size distribution. To our knowledge, LDSA size distributions for wood and MSW combustion has not been published in peer-reviewed literature. Similar bimodal LDSA size distribution, with median sizes between 190 and 410 nm, has been observed by Salo et al. (2021) during a long-range pollution event in Helsinki and in the highly polluted Delhi-National Capital Region. Inline with our results, Kuuluvainen et al. (2016) observed that the ambient LDSA size distribution maximum was around 100 nm for traffic influenced areas and around 200 nm in measurements conducted in residential areas. The inhalation, toxicity and thus health impacts of particles are strongly connected to both the average size and the surface area and thus it is very important to measure the particle size distribution and LDSA in addition to PM concentration in order to enhance the understanding of how particles impact our health.

3.4. Influence of MSW to particle composition

Fig. 5 presents the average composition of submicron particles for each phase measured during cycles 1–5 (upper panel) and the contribution (%) of the major chemical constituents (lower panel) measured with the SP-AMS. The PAM chamber was used to simulate the secondary aerosol formation potential, i.e., the effects of atmospheric ageing on mass concentrations and composition of emitted aerosol. Phases where the PAM chamber has been used are marked to figure with the text 'PAM' and phases where wood + MSW were burned marked with 'MSW'.

In general, the main components of submicron PM in flue gas were organics and rBC (Fig. 4). When compared to wood, the wood + MSW combustion clearly increased rBC concentration (65%) and slightly decreased the concentration of organic compounds (26%). Similar PM composition for wood combustion has been observed e.g. by Frey et al. (2009) and Kortelainen et al. (2018). However, in this study large variations were observed between different burning phases but the PM concentrations were quite similar between the cycles.

During the ignition periods the major particulate components were organic compounds (20%) and refractive black carbon (rBC, 78%), together representing on average 99% of mass. Ignition of wood + MSW mixture did not cause significant increases to the emissions of the main components or the composition of PM during ignition. In the case of aged emissions (after the PAM chamber) the contribution of organics increased (50%), but in general secondary PM emissions were on the same level during ignition as the primary emissions, indicating that secondary aerosol formation was not significant during ignition.

During the burning phases, large variation in submicron PM emissions was observed, however, the primary emissions for wood and wood + MSW were quite similar from the particle composition perspective and in general the concentrations of fresh emissions were slightly lower than during ignition period (Fig. 4). During the burning, organics and rBC were the main contributors to PM mass, however the contribution of inorganic compounds to submicron particulate mass slightly increased but still remained at low level. Similar to burning, large variation in submicron PM emissions was observed for burning end phases. The chemical composition measurement showed that the contribution of organics was larger during burning end phase than during the burning phase. The aging of flue gases in the PAM chamber increased the mass of

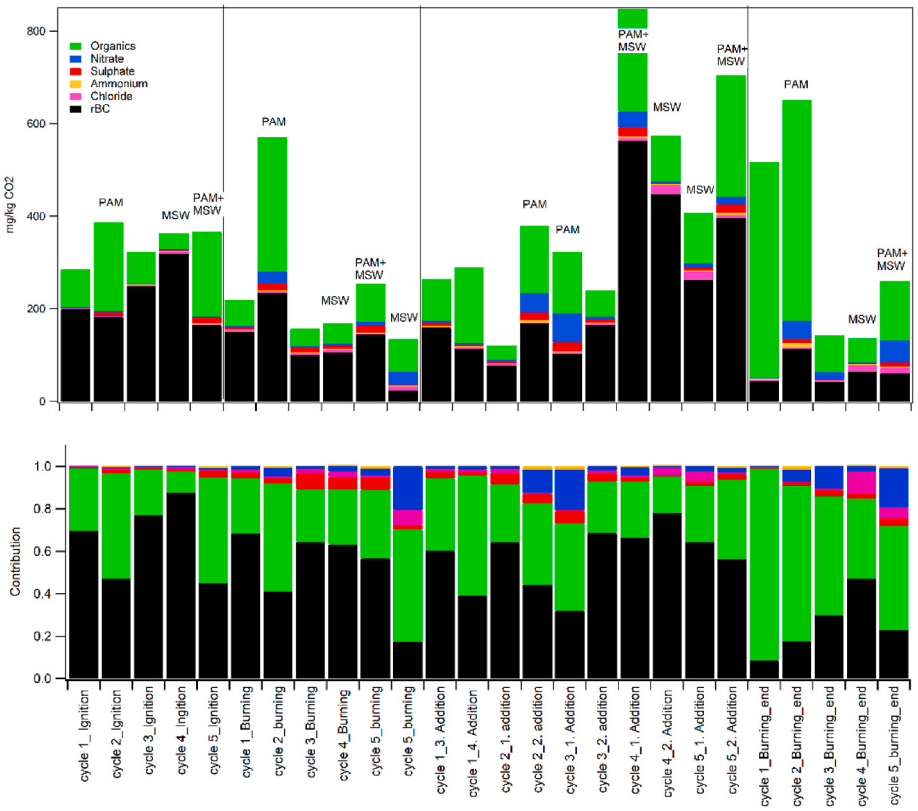

Fig. 5. Average mass concentrations of rBC, organics, nitrate, sulphate, ammonium and chloride of submicron particulate emissions (upper panel) and average contribution of each chemical constituent (lower panel) for each phases of cycles. The measurement phases where PAM has been applied are marked with "PAM" and phases where MSW was burned marked with "MSW". The composition was measured with SP-AMS and the values are normalized with CO_2.

particulate organics, both for wood burning and wood + MSW burning.

Similarly, as was observed for size distributions, the MSW had a major influence on concentration and composition of submicron particulate emissions during fuel additions. Significant increase was seen both in rBC (275% increase) and organic concentrations (20% increase) of fresh flue gas and in organic concentration of flue gas treated by PAM chamber.

BC forms in incomplete combustion and observed increase in BC emission indicates that MSW changed the combustion conditions. Frey et al. observed over 50% increase in EC when combustion conditions were changed from good to smoldering combustion.

Inline with our results, Stockwell et al. (2016), observed higher BC emission factors for emissions of mixed waste burning from open fires compared to other fuels. Also, previous studies have indicated that organic fraction from waste combustion typically contains for example PAH and BTEX compounds (e.g. Stockwell et al., 2016; Hoffer et al., 2020) that are known to be detrimental for health (Schwarze et al., 2006) and therefore, the change in composition by MSW combustion is rather concerning.

Related to wood burning, the mean ratios of organic to rBC were on average between 0.27 and 4.48 depending on the burning phase and aging. The MSW addition was not observed to have systematic influence on organic to rBC -ratios. Fig. S9 shows the organic to rBC -ratios for each phase in each cycle. Observed ratios are lower than in Grieshop et al. (2009) who found organic to BC ratios ranging from 1.1 to 13 for fresh wood combustion emissions. Our results were also smaller when compared to ratios observed for flex-fuel vehicles (0.9–3.1 (Timonen et al., 2017);) or in the atmosphere (1.5–20; (Aurela et al., 2011). In general, the PAM enhancement ratios (ER) were relatively low (1.7–3), as typically observed for wood combustion (Ortega et al., 2013).

3.5. Trace metal emissions during the fuel additions

Fig. 6 shows the "wood + MSW combustion to wood combustion" -ratio for different trace metals and their salts (Al, Cd, Fe, Nb, Rh, Sb, Zn, HCl, KCl, NaCl) during the different burning phases.

For wood burning the trace metal emissions were relatively low, but significant increase (on average 3.3–179 -fold increase over cycle) was seen when MSW was added along the wood. High ratios were observed especially during fuel addition phases but, depending on compounds, also during ignition and burning end phases (Fig. 6). The highest ratios were observed for chloride compounds (HCl, KCl, NaCl). Potassium and chlorine content in the wood varies between different wood species and the geographical location of the trees (Shah et al., 2010; Jenkins et al., 1998). When wood is combusted, potassium, sodium and chloride are released from the fuel (Sorvajärvi et al., 2014). They form potassium chloride (KCl) and sodium chloride (NaCl) in the gas phase both of which can cause corrosion in fireplaces (Skrifvars et al., 2008). The KCl release from wood combustion and water in the gas phase react together releasing HCl (Lehmusto et al., 2019). Kortelainen et al. (2018) also observed Cl, Zn, Na, Fe and K emissions when burning spruce, beech and birch. The elevated chloride compound concentrations during MSW burning indicate that either the MSW also released additional chloride compounds to flue gas or changed the chemistry to favor gas-to-particle phase change of chloride compounds. Elevated ambient chloride compounds from combustion of biomass and likely mixed waste are typically observed in polluted areas such as India (Gani et al., 2019; Gunthe et al., 2021). Gunthe et al. (2021) found that highly water-absorbing and soluble chloride in the aqueous phase substantially enhances aerosol water uptake through co-condensation, which sustains particle growth and leads to haze and fog formation. Their results suggest that the high local concentration of gas-phase hydrochloric acid causes some 50% of the reduced visibility.

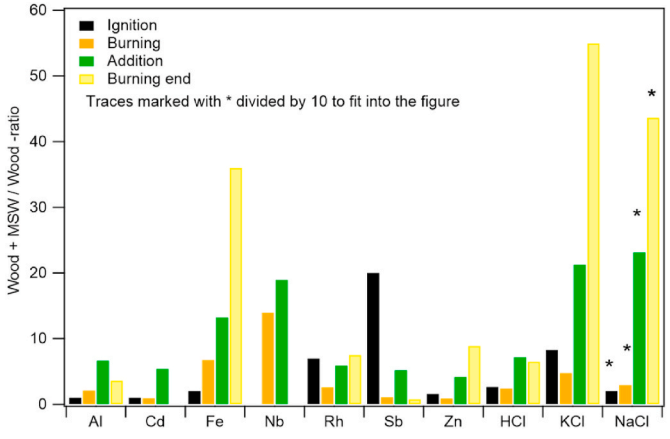

Fig. 6. The average Wood + MSW/Wood -ratios for different metals and their salts measured with SP-AMS for ignition, addition, burning and burning end phases. The ratios for NaCl (marked with *) were divided by 10 to fit data into the same scale.

In addition to chloride compounds, we observed elevated concentrations of a variety of other metals (Al, Cd, Fe, Nb, Rh, Sb, Zn) in flue gas when MSW was burned. Many of metals observed in this study (e.g. Al, Fe, Cd, K) are also found naturally in wood and bark (Chandrasekaran et al., 2012). However, the higher concentrations observed for MSW burning indicate that the origin of these metals is likely MSW materials, including e.g. paints, foil-coatings, additives, stabilizers, fire retardants and color pigments used in variable roles and concentrations in cardboard, wood, textiles and plastic products. Trace metals, such as antimony, have been proposed as a tracers for waste combustion. Christian et al. (2010) measured metal emissions from variety of sources (e.g. indoor open wood cooking fires, charcoal and brick making kilns, garbage burns in peri-urban landfills and barley stubble field burns) in Mexico. They observed over 300 times higher antimony emissions for garbage burning than for crop burning. Also, Jayarathne et al. (2018) observed that garbage burning emissions from open fires contained relatively high concentrations of heavy metals (Cu, Pb, Sb). Our results for antimony, showing significant increase especially during ignition and fuel additions, are in line with the previous results and further confirm that the antimony could be a good tracer for MSW combustion emissions.

Metals in wood combustion derived aerosols have known effects for toxicity (e.g. Uski et al., 2015; Kocbach Bolling et al., 2009) and therefore, it may be anticipated that MSW burning is increasing those effects due to larger concentrations.

4. Conclusions

Although it is mostly forbidden, household waste is often burned with wood to reduce the cost of heating and to dispose the waste, even in developed countries. In this study, wood and wood mixed with household waste were burnt in a masonry heater to characterize the influence of waste combustion to particulate emissions in the flue gas. Household waste combustion along with wood in a stove appliance commonly used in the households was observed to increase the particulate emissions. The most pronounced effects were seen during the fuel addition periods, when the concentrations of PN, PM, BC and LDSA increased and mean particle size increased. Especially, the increased metal concentrations combined with increased lung deposition surface area indicate that waste burning could potentially have influences to human health.

Furthermore, the increase in chloride emissions due to MSW burning will likely have negative impact to condition of burning device due to corrosion. The increase of particulate emissions will likely affect the air quality in nearby areas and houses. In addition, both the BC and metals absorb light and thus warm climate and change the albedo of snow and ice surfaces causing melting.

Credit author roles

Hilkka Timonen: Writing -Original draft, review and editing, Analysis and interpretation of data, Visualization, supervision. Fanni Mylläri: Conception and design of the study, Acquisition of data, Analysis of data, Writing - review and editing. Pauli Simonen: Acquisition of data, Analysis of data, Writing - review and editing. Minna Aurela: Acquisition of data, Analysis of data, Writing - review and editing. Marek Maasikmets: Methodology, Conception and design of the study, Acquisition of data, Analysis of data, Writing - review and editing, Matthew Bloss: Acquisition of data, Analysis and interpretation of data, Writing original draft, Visualization. Hanna-Lii, Kupri: Acquisition of data, Writing - review and editing, Keio Vainumäe: Methodology, Conception and design of the study, Analysis and interpretation of data, Writing - review and editing, Funding acquisition. Teemu Lepistö: Acquisition of data, analysis of data, Writing - review and editing. Laura Salo: Acquisition of data, Analysis of data, Writing - review and editing, Ville Niemelä: Analysis and interpretation of data, Acquisition of data, Funding acquisition, Writing - review and editing, Sami Seppälä: Analysis and interpretation of data, Writing - review and editing. Pasi. I. Jalava: Analysis and interpretation of data, Writing - review and editing, Erik Teinemaa: Methodology, Conception and design of the study, Analysis and interpretation of data, Writing - review and editing, Funding acquisition. Sanna Saarikoski: Analysis and interpretation of data, Writing - review and editing, Funding acquisition. Topi Rönkkö: Methodology, Conception and design of the study, Analysis and interpretation of data, Writing - review and editing, Funding acquisition, supervision.

Declaration of competing interest

The authors declare that they have no known competing financial interests or personal relationships that could have appeared to influence the work reported in this paper.

Acknowledgements

This work was supported by the Estonian Environmental Investment Centre project no. 10627, BC Footprint project (528/31/2019) funded by Business Finland and participating companies and Strategic Research Council at the Academy of Finland, project Transition to a resource efficient and climate neutral electricity system (EL-TRAN, grant number 314319*)* and Academy of Finland Flagship funding (grant no. 337552, 337551).

Appendix A. Supplementary data

Supplementary data to this article can be found online at https://doi.org/10.1016/j.jenvman.2021.112793.

References

Argyropoulos, G., Manoli, E., Kouras, A., Samara, C., 2012. Concentrations and source apportionment of PM10 and associated major and trace elements in the Rhodes Island, Greece. Sci. Total Environ. 432, 12–22. https://doi.org/10.1016/j.scitotenv.2012.05.076.

Aurela, M., Saarikoski, S., Timonen, H., Aalto, P., Keronen, P., Saarnio, K., Teinilä, K., Kulmala, M., Hillamo, R., 2011. Carbonaceous aerosol at a forested and an urban background sites in Southern Finland. Atmos. Environ. 45, 1394–1401. https://doi.org/10.1016/j.atmosenv.2010.12.039.

Carbone, S., Onasch, T., Saarikoski, S., Timonen, H., Saarnio, K., Sueper, D., Rönkkö, T., Pirjola, L., Häyrinen, A., Worsnop, D., Hillamo, R., 2015. Characterization of trace metals on soot aerosol particles with the SP-AMS: detection and quantification. Atm. Meas. Tech. 8, 4803–4815. https://doi.org/10.5194/amt-8-4803-2015.

Chandrasekaran, S.R., Hopke, P.K., Rector, L., Allen, G., Lin, L., 2012. Chemical composition of wood chips and wood pellets. Energy Fuels 26, 4932–4937. https://doi.org/10.1021/ef300884k.

Chen, J., Li, C., Ristovski, Z., Milic, A., Gu, Y., Islam, M.S., Wang, S., Hao, J., Zhang, H., He, C., Guo, H., Fu, H., Miljevic, B., Morawska, L., Thai, P., Lam, Y.F., Pereira, G., Ding, A., Huang, X., Dumka, U.C., 2017. A review of biomass burning: emissions and impacts on air quality, health and climate in China. Sci. Total Environ. 579, 1000–1034. https://doi.org/10.1016/j.scitotenv.2016.11.025.

Cheristanidis, S., Grivas, G., Chaloulakou, A., 2020. Determination of total and lung-deposited particle surface area concentrations, in central Athens, Greece. Environ. Monit. Assess. t 192 (627). https://doi.org/10.1007/s10661-020-08569-8.

Christian, T.J., Yokelson, R.J., Cardenas, B., Molina, L.T., Engling, G., 2010. Trace Gas and Particle Emissions from Domestic and Industrial Biofuel Use and Garbage Burning in Central Mexico, vol. 20.

Cubison, M.J., Ortega, A.M., Hayes, P.L., Farmer, D.K., Day, D., Lechner, M.J., Brune, W. H., Apel, E., Diskin, G.S., Fisher, J.A., Fuelberg, H.E., Hecobian, A., Knapp, D.J., Mikoviny, T., Riemer, D., Sachse, G.W., Sessions, W., Weber, R.J., Weinheimer, A.J., Wisthaler, A., Jimenez, J.L., 2011. Effects of aging on organic aerosol from open biomass burning smoke in aircraft and laboratory studies. Atmos. Chem. Phys. 11, 12049–12064. https://doi.org/10.5194/acp-11-12049-2011.

DeCarlo, P.F., Ulbrich, I.M., Crounse, J., de Foy, B., Dunlea, E.J., Aiken, A.C., Knapp, D., Weinheimer, A.J., Campos, T., Wennberg, P.O., Jimenez, J.L., 2010. Investigation of the sources and processing of organic aerosol over the Central Mexican Plateau from aircraft measurements during MILAGRO. Atmos. Chem. Phys. 10, 5257–5280. https://doi.org/10.5194/acp-10-5257-2010.

Forouzanfar, M.H., Alexander, L., Anderson, H.R., Bachman, V.F., Biryukov, S., Brauer, M., Murray, C.J., et al., 2015. Global, regional, and national comparative risk assessment of79 behavioural, environmental and occupational, and metabolic risks or clusters of risks in 188 countries, 1990–2013: a systematic analysis for the global burden of disease study 2013. Lancet 386, 2287–2323. https://doi.org/10.1016/S0140-6736(15)00128-2.

Frey, A.K., Tissari, J., Saarnio, K.M., Timonen, H.J., Tolonen-Kivimäki, O., Aurela, M.A., Saarikoski, S.K., Makkonen, U., Hytönen, K., Jokiniemi, J., Salonen, R.O., Hillamo, R.E.J., 2009. Chemical composition and mass size distribution of fine particulate matter emitted by a small masonry heater. Boreal Environ. Res. 14, 255–271.

Gangwar, C., Choudhari, R., Chauhan, A., Kumar, A., Singh, A., Tripathi, A., 2019. Assessment of air pollution caused by illegal e-waste burning to evaluate the human health risk. Environ. Int. 125, 191–199. https://doi.org/10.1016/j.envint.2018.11.051.

Gani, S., Bhandari, S., Seraj, S., Wang, D.S., Patel, K., Soni, P., Arub, Z., Habib, G., Hildebrandt Ruiz, L., Apte, J.S., 2019. Submicron aerosol composition in the world's most polluted megacity: the Delhi Aerosol Supersite study. Atmos. Chem. Phys. 19, 6843–6859. https://doi.org/10.5194/acp-19-6843-2019.

Grieshop, A.P., Donahue, N.M., Robinson, A.L., 2009. Laboratory investigation of photochemical oxidation of organic aerosol from wood fires 2: analysis of aerosol mass spectrometer data. Atmos. Chem. Phys. 9, 2227–2240. https://doi.org/10.5194/acp-9-2227-2009.

Gunthe, S.S., Liu, P., Panda, U., et al., 2021. Enhanced aerosol particle growth sustained by high continental chlorine emission in India. Nat. Geosci. 14, 77–84. https://doi.org/10.1038/s41561-020-00677-x.

Hedman, B., Näslund, M., Marklund, S., 2006. Emission of PCDD/F, PCB, and HCB from combustion of firewood and pellets in residential stoves and boilers. Environ. Sci. Technol. 40, 4968–4975. https://doi.org/10.1021/es0524189.

Helin, A., Niemi, J.V., Virkkula, A., Pirjola, L., Teinilä, K., Backman, J., Aurela, M., Saarikoski, S., Rönkkö, T., Asmi, E., Timonen, H., 2018. Characteristics and source apportionment of black carbon in the Helsinki metropolitan area. Finland, Atmos. Environ. 190, 87–98. https://doi.org/10.1016/j.atmosenv.2018.07.022.

Hennigan, C.J., Miracolo, M.A., Engelhart, G.J., May, A.A., Presto, A.A., Lee, T., Sullivan, A.P., McMeeking, G.R., Coe, H., Wold, C.E., Hao, W.-M., Gilman, J.B., Kuster, W.C., de Gouw, J., Schichtel, B.A., Collett, J.L., Kreidenweis, S.M., Robinson, A.L., 2011. Chemical and physical transformations of organic aerosol from the photo-oxidation of open biomass burning emissions in an environmental chamber. Atmos. Chem. Phys. 11, 7669–7686. https://doi.org/10.5194/acp-11-7669-2011.

Hoffer, A., Jancsek-Turóczi, B., Tóth, Á., Kiss, G., Naghiu, A., Levei, E.A., Marmureanu, L., Machon, A., Gelencsér, A., 2020. Emission factors for PM10 and PAHs from illegal burning of different types of municipal waste in households. Atmos. Chem. Phys. Discuss. https://doi.org/10.5194/acp-2020-672 submitted for publication.

Hosseini, S., Li, Q., Cocker, D., Weise, D., Miller, A., Shrivastava, M., Miller, J.W., Mahalingam, S., Princevac, M., Jung, H., 2010. Particle size distributions from laboratory-scale biomass fires using fast response instruments. Atmos. Chem. Phys. 10, 8065–8076. https://doi.org/10.5194/acp-10-8065-2010.

Ihalainen, M., Tiitta, P., Czech, H., Yli-Pirilä, P., Hartikainen, A., Kortelainen, M., Tissari, J., Stengel, B., Sklorz, M., Suhonen, H., Lamberg, H., Leskinen, A., Kiendler-Scharr, A., Harndorf, H., Zimmermann, R., Jokiniemi, J., Sippula, O., 2019. A novel high-volume Photochemical Emission Aging flow tube Reactor (PEAR). Aerosol Sci. Technol. 53, 276–294. https://doi.org/10.1080/02786826.2018.1559918.

IPCC, 2013. Climate Change 2013: the Physical Science Basis. Contribution of Working Group I to the Fifth Assessment Report of the Intergovernmental Panel on Climate Change. Cambridge University Press. https://doi.org/10.1017/cbo9781107415324.

Jalava, P.I., Happo, M.S., Kelz, J., Brunner, T., Hakulinen, P., Mäki-Paakkanen, J., Hukkanen, A., Jokiniemi, J., Obernberger, I., Hirvonen, M.-R., 2012. In vitro toxicological characterization of particulate emissions from residential biomass heating systems based on old and new technologies. Atmos. Environ. 50, 24–35.

Janssen, N.A., Hoek, G., Simic-Lawson, M., Fischer, P., van Bree, L., ten Brink, H., Keuken, M., Atkinson, R.W., Anderson, H.R., Brunekreef, B., Cassee, F.R., 2011. Black carbon as an additional indicator of the adverse health effects of airborne particles compared with PM10 and PM2.5. Environ. Health Perspect. 119, 1691–1699. https://doi.org/10.1289/ehp.1003369.

Järvinen, A., Aitomaa, M., Rostedt, A., Keskinen, J., Yli-Ojanperä, J., 2014. Calibration of the new electrical low pressure impactor (ELPI+). J. Aerosol Sci. 69, 150–159. https://doi.org/10.1016/j.jaero-sci.2013.12.006.

Järvinen, A., Timonen, H., Karjalainen, P., Bloss, M., Simonen, P., Saarikoski, S., Kuuluvainen, H., Kalliokoski, J., Dal Maso, M., Niemi, J.V., Keskinen, J., Rönkkö, T., 2019. Particle emissions of Euro VI, EEV and retrofitted EEV city buses in real traffic. Env. pollut 250, 708–716. https://doi.org/10.1016/j.envpol.2019.04.033.

Jayarathne, T., Stockwell, C.E., Bhave, P.V., Praveen, P.S., Rathnayake, C.M., Islam, Md R., Panday, A.K., Adhikari, S., Maharjan, R., Goetz, J.D., DeCarlo, P.F., Saikawa, E., Yokelson, R.J., Stone, E.A., 2018. Nepal Ambient Monitoring and Source Testing Experiment (NAMaSTE): emissions of particulate matter from wood- and dung-fueled cooking fires, garbage and crop residue burning, brick kilns, and other sources. Atmos. Chem. Phys. 18, 2259–2286. https://doi.org/10.5194/acp-18-2259-2018.

Jenkins, B.M., Baxter, L.L., Miles Jr., T.R., Miles, T.R., 1998. Combustion properties of biomass, fuel process. Technol. 54 17–46.

Jimenez, J.L., Canagaratna, M.R., Donahue, N.M., Prévôt, A.S.H., Zhang, Q., Kroll, J.H., DeCarlo, P.F., Allan, J.D., Coe, H., Ng, N.L., Aiken, A.C., Docherty, K.S., Ulbrich, I. M., Grieshop, A.P., Robinson, A.L., Duplissy, J., Smith, J.D., Wilson, K.R., Lanz, V.A., Hueglin, C., Sun, Y.L., Tian, J., Laaksonen, A., Raatikainen, T., Rautiainen, J., Vaattovaara, P., Ehn, M., Kulmala, M., Tomlinson, J.M., Collins, D.R., Cubison, M.J., Dunlea, E.J., Huffman, J.A., Onasch, T.B., Alfarra, M.R., Williams, P.I., Bower, K., Kondo, Y., Schneider, J., Drewnick, F., Borrmann, S., Weimer, S., Demerjian, K., Salcedo, D., Cottrell, L., Griffin, R., Takami, A., Miyoshi, T., Hatakeyama, S., Shimono, A., Sun, J.Y., Zhang, Y.M., Dzepina, K., Kimmel, J.R., Sueper, D., Jayne, J. T., Herndon, S.C., Trimborn, A.M., Williams, L.R., Wood, E.C., Middlebrook, A.M., Kolb, C.E., Baltensperger, U., Worsnop, D.R., 2009. Evolution of organic aerosols in the atmosphere. Science 326, 1525–1529. https://doi.org/10.1126/science.1180353.

Kang, E., Root, M.J., Toohey, D.W., Brune, W.H., 2007. Introducing the concept of potential aerosol mass (PAM). Atmos. Chem. Phys. 7, 5727–5744. https://doi.org/10.5194/acp-7-5727-2007.

Kang, E., Toohey, D.W., Brune, W.H., 2011. Dependence of SOA oxidation on organic aerosol mass concentration and OH exposure: experimental PAM chamber studies. Atmos. Chem. Phys. 11, 1837–1852. https://doi.org/10.5194/acp-11-1837-2011.

Kasurinen, S., Uski, O., Jalava, P.I., Brunner, T., Happo, M.S., Mäki-Paakkanen, J., Jokiniemi, J., Obernberger, I., Hirvonen, M.-R., 2016. Toxicological characterization of particulate emissions from straw, mischantus and poplar pellet combustion in residential boilers. Aerosol Sci. Technol. 50, 41–51.

Keskinen, J., Pietarinen, K., Lehtimäki, M., 1992. Electrical low pressure impactor. J. Aerosol Sci. 23, 353–360. https://doi.org/10.1016/0021-8502(92)90004-F.

Kocbach Bolling, A., Pagels, J., Yttri, K.E., Barregård, L., Sällsten, G., Schwarze, P.E., Boman, C., 2009. Health effects of residential wood smoke particles: the importance of combustion conditions and physicochemical particle properties, Part. Fibre Toxicol 6 (29).

Kortelainen, M., Jokiniemi, J., Nuutinen, I., Torvela, T., Lamberg, H., Karhunen, T., Tissari, J., Sippula, O., 2015. Ash behaviour and emission formation in a small-scale reciprocating-grate combustion reactor operated with wood chips, reed canary grass and barley straw. Fuel 143, 80–88. https://doi.org/10.1016/j.fuel.2014.11.006.

Kortelainen, M., Jokiniemi, J., Tiitta, P., Tissari, J., Lamberg, H., Leskinen, J., Grigonyte-Lopez Rodriguez, J., Koponen, H., Antikainen, S., Nuutinen, I., Zimmermann, R., Sippula, O., 2018. Time-resolved chemical composition of small-scale batch combustion emissions from various wood species. Fuel 233, 224–236. https://doi.org/10.1016/j.fuel.2018.06.056.

Kroll, J.H., Seinfeld, J.H., 2008. Chemistry of secondary organic aerosol: formation and evolution of low-volatility organics in the atmosphere. Atmos. Environ. 42, 3593–3624. https://doi.org/10.1016/j.atmosenv.2008.01.003.

Kuuluvainen, H., Rönkkö, T., Järvinen, A., Saari, S., Karjalainen, P., Lähde, T., Pirjola, L., Niemi, J.V., Hillamo, R., Keskinen, J., 2016. Lung deposited surface area size distributions of particulate matter in different urban areas. Atmos. Environ. 136, 105–113. https://doi.org/10.1016/j.atmosenv.2016.04.019.

Lambe, A.T., Ahern, A.T., Williams, L.R., Slowik, J.G., Wong, J.P.S., Abbatt, J.P.D., Brune, W.H., Ng, N.L., Wright, J.P., Croasdale, D.R., Worsnop, D.R., Davidovits, P., Onasch, T.B., 2011. Characterization of aerosol photooxidation flow reactors: heterogeneous oxidation, secondary organic aerosol formation and cloud condensation nuclei activity measurements. Atm. Meas. Tech. 4, 445–461. https://doi.org/10.5194/amt-4-445-2011.

Lambe, A.T., Chhabra, P.S., Onasch, T.B., Brune, W.H., Hunter, J.F., Kroll, J.H., Cummings, M.J., Brogan, J.F., Parmar, Y., Worsnop, D.R., Kolb, C.E., Davidovits, P., 2015. Effect of oxidant concentration, exposure time, and seed particles on secondary organic aerosol chemical composition and yield. Atmos. Chem. Phys. 15, 3063–3075. https://doi.org/10.5194/acp-15-3063-2015.

Lehmusto, J., Olin, M., Viljanen, J., Kalliokoski, J., Mylläri, F., Toivonen, J., Dal Maso, M., Hupa, L., 2019. Detection of Gaseous Species during KCl-Induced High-Temperature Corrosion by the Means of CPFAAS and CI-APi-TOF, Materials and Corrosion. https://doi.org/10.1002/maco.201910964.

Lelieveld, J., Evans, J.S., Fnais, M., Giannadaki, D., Pozzer, A., 2015. The contribution of outdoor air pollution sources to premature mortality on a global scale. Nature 525, 367–371. https://doi.org/10.1038/nature15371.

Lepistö, T., Kuuluvainen, H., Juuti, P., Järvinen, A., Arffman, A., Rönkkö, T., 2020. Measurement of the human respiratory tract deposited surface area of particles with an electrical low pressure impactor. Aerosol Sci. Technol. https://doi.org/10.1080/02786826.2020.1745141.

Lim, S.S., Vos, T., Flaxman, A.D., Danaei, G., Shibuya, K., Adair-Rohani, H., Ezzati, M., et al., 2012. A comparative risk assessment of burden of disease and injury attributable to 67 risk factors and risk factor clusters in 21 regions, 1990–2010: a systematic analysis for the global burden of disease study 2010. Lancet 380, 2224–2260.

Liu, Peter S. K., Rensheng Deng, Kenneth A. Smith, Leah R. Williams, John T. Jayne, Manjula R. Canagaratna, Kori Moore, Timothy B. Onasch, Douglas R. Worsnop, and Terry Deshler. "Transmission Efficiency of an Aerodynamic Focusing Lens System: Comparison of Model Calculations and Laboratory Measurements for the Aerodyne Aerosol Mass Spectrometer." Aerosol. Sci. Technol. , 41, 721-733, https://doi.org/10.1080/02786820701422278.

Maasikmets, M., 2019. Determination of Emission Factors from Anthropogenic Particle Sources for Air Emission and Health Impact Assessment. https://doi.org/10.15159/emu.37.

Maasikmets, M., Kupri, H.-L., Teinemaa, E., Vainumäe, K., Arumäe, T., Kimmel, V., 2015. ACSM study to assess possible municipal solid waste burning in household stoves. In: European Aerosol Conference. https://doi.org/10.13140/RG.2.1.2100.0167.

Maasikmets, M., Kupri, H.-L., Teinemaa, E., Vainumäe, K., Arumäe, T., Roots, O., Kimmel, V., 2016. Emissions from burning municipal solid waste and wood in domestic heaters. Atmos. Pollut. Res 7, 438–446. https://doi.org/10.1016/j.apr.2015.10.021.

Marjamäki, M., Keskinen, J., Chen, D., Pui, D.Y.H., 2000. Performance evaluation of the electrical low pressure impactor (ELPI). J. Aerosol Sci. 31 (2), 249–261. https://doi.org/10.1016/S0021-8502(99)00052-X.

Marjamäki, M., Ntziachristos, L., Virtanen, A., Ristimäki, J., Keskinen, J., Moisio, M., Palonen, M., Lappi, M., 2002. Electrical Filter Stage for the ELPI, SAE Technical Paper Series, 2002-01-0055.

Meallem, I., Garb, Y., Cwikel, J., 2010. Environmental hazards of waste disposal patterns - a multimethod study in an unrecognized Bedouin village in the Negev area of Israel. Arch. Environ. Occup. Health 65 (4), 230–237. https://doi.org/10.1080/19338244.2010.486426.

Menezes-Filho, J.A., De Sousa Viana, G.F., Paes, C.R., 2012. Determinants of lead exposure in children on the outskirts of Salvador, Brazil. Environ. Monit. Assess. 184, 2593–2603.

Middlebrook, A.M., Bahreini, R., Jimenez, J.L., Canagaratna, M.R., 2012. Evaluation of composition-dependent collection efficiencies for the Aerodyne aerosol mass spectrometer using field data. Aerosol Sci. Technol. 46, 258–271. https://doi.org/10.1080/02786826.2011.620041.

Muala, A., Rankin, G., Sehlstedt, M., Unosson, J., Bosson, J.A., Behndig, A., Pourazar, J., Nyström, R., Pettersson, E., Bergwall, C., Westerholm, R., Jalava, P.I., Happo, M.S., Uski, O., Hirvonen, M.-R., Kelly, F.J., Mudway, I.S., Blomberg, A., Boman, C., Sandström, T., 2015. Acute exposure to wood smoke from incomplete combustion – indications of cytotoxicity, Part. Fibre Toxicol 12.

Ohtonen, K., Kaski, N., Niemi, J., 2018. Use of fireplaces: emissions in the Helsinki metropolitan area. In: 2018, Helsinki Region Environmental Services Authority (HSY) Report (In Finnish), p. 51. ISSN (online): 1798-6095. https://julkaisu.hsy.fi/tulisijojen-kaytto-ja-paastot-paakaupunkiseudulla-vuonna-2018.pdf.

Onasch, T.B., Trimborn, A., Fortner, E.C., Jayne, J.T., Kok, G.L., Williams, L.R., Davidovits, P., Worsnop, D.R., 2012. Soot particle aerosol mass spectrometer: development, validation, and initial application. Aerosol Sci. Technol. 46, 804–817. https://doi.org/10.1080/02786826.2012.663948.

Ortega, A., Day, D.A., Cubison, M.J., Brune, W.H., Bon, D., de Gouw, J.A., Jimenez, J.L., 2013. Secondary organic aerosol formation and primary organic aerosol oxidation from biomass-burning smoke in a flow reactor during FLAME-3. Atmos. Chem. Phys. 13, 11551–11571. https://doi.org/10.5194/acp-13-11551-2013.

Ortega, A.M., Hayes, P.L., Peng, Z., Palm, B.B., Hu, W., Day, D.A., Li, R., Cubison, M.J., Brune, W.H., Graus, M., Warneke, C., Gilman, J.B., Kuster, W.C., de Gouw, J., Gutiérrez-Montes, C., Jimenez, J.L., 2016. Real-time measurements of secondary organic aerosol formation and aging from ambient air in an oxidation flow reactor in the Los Angeles area. Atmos. Chem. Phys. 16, 7411–7433. https://doi.org/10.5194/acp-16-7411-2016.

Patel, S., LEavey, A., Sheshadri, A., Kumar, P., Kandikuppa, S., Tarsi, J., Mukhopadhyay, K., Johnson, P., Balakrishnan, K., Schechtman, K.B., Yadama, G., Biswas, P., 2018. Associations between household air pollution and reduced lung function in women and children in rural southern India. J. Appl. Toxicol. 38.

Pokhrel, R.P., Gordon, J., Fiddler, M.N., Bililign, S., 2021. Impact of combustion conditions on physical and morphological properties of biomass burning aerosol. Aerosol. Sci. Technol. 55 (1), 80–91. https://doi.org/10.1080/02786826.2020.1822512.

Rivellini, L.H., Chiapello, I., Tison, E., Fourmentin, M., Feron, A., Diallo, A., N'Diaye, T., Goloub, P., Canonaco, F., Prevet, A.S.H., Riffault, V., 2017. Chemical characterization and source apportionment of submicron aerosols measured in Senegal during the 2015 SHADOW campaign. Atmos. Chem. Phys. 17, 10291–10314.

Rönkkö, T., Kuuluvainen, H., Karjalainen, P., Keskinen, J., Hillamo, R., Niemi, J.V., Pirjola, L., Timonen, H.J., Saarikoski, S., Saukko, E., Järvinen, A., Silvennoinen, H., Rostedt, A., Olin, M., Yli-Ojanperä, J., Nousiainen, P., Kousa, A., Dal Maso, M., 2017. Traffic is a major source of atmospheric nanocluster aerosol. Proc. Natl. Acad. Sci. Unit. States Am., 201700830 https://doi.org/10.1073/pnas.1700830114.

Salo, L., Mylläri, F., Maasikmets, M., Niemelä, V., Konist, A., Vainumäe, K., Kupri, H.-L., Titova, R., Simonen, P., Aurela, M., Bloss, M., Keskinen, J., Timonen, H., Rönkkö, T., 2019. Emission measurements with gravimetric impactors and electrical devices: an aerosol instrument comparison. Aerosol. Sci. Technol. 53, 526–539. https://doi.org/10.1080/02786826.2019.1578858.

Salo, L., Hyvärinen, A., Jalava, P., Teinilä, K., Hooda, R.K., Datta, A., Saarikoski, S., Lintusaari, H., Lepistö, T., Martikainen, S., Rostedt, A., Sharma, V.P., Rahman, MdH., Subudhi, S., Asmi, E., Niemi, J.V., Lihavainen, H., Lal, B., Keskinen, J., Kuuluvainen, H., Timonen, H., Rönkkö, T., 2021. The Characteristics and Size of Lung-Depositing Particles Vary Significantly between High and Low Pollution Traffic

Environments. Atmospheric Environment. https://doi.org/10.1016/j.atmosenv.2021.118421 (in press).
Savolahti, M., Karvosenoja, N., Tissari, J., Kupiainen, K., Sippula, O., Jokiniemi, J., 2016. Black carbon and fine particle emissions in Finnish residential wood combustion: emission projections, reduction measures and the impact of combustion practices. Atmos. Environ. 140, 495–505. https://doi.org/10.1016/j.atmosenv.2016.06.023.
Savolahti, M., Karvosenoja, N., Soimakallio, S., Kupiainen, K., Tissari, J., Paunu, V.-V., 2019. Near-term climate impacts of Finnish residential wood combustion. Energy Pol. 133, 110837 https://doi.org/10.1016/j.enpol.2019.06.045.
Schwarze, P.E., Ovrevik, J., Låg, M., Refsner, M., Nafstad, P., Hetland, R.B., Dybing, E., 2006. Particulate matter properties and health effects: consistency of epidemiological and toxicological studies. Hum. Exp. Toxicol. 25, 559–579.
Stockholm Environment Institute, SEI, 2013. Tallinn, uuringu lõpparuanne. In: Eestis Tekkinud Segaolmejäätmete, Eraldi Kogutud Paberi- Ja Pakendijäätmete Ning Elektroonikaromu Koostise Uuring, p. 52. https://www.envir.ee/sites/default/files/sortimisuuring_2013loplik.pdf.
Shah, K.V., Cieplik, M.K., Betrand, C.I., van de Kamp, W.L., Vuthaluru, H.B., 2010. Correlating the effects of ash elements and their association in the fuel matrix with the ash release during pulverized fuel combustion. Fuel Process. Technol. 91, 531–545. https://doi.org/10.1016/j.fuproc.2009.12.016.
Simonen, P., Saukko, E., Karjalainen, P., Timonen, H., Bloss, M., Aakko-Saksa, P., Rönkkö, T., Keskinen, J., Dal Maso, M., 2017. A new oxidation flow reactor for measuring secondary aerosol formation of rapidly changing emission sources. Atm. Meas. Tech. 10, 1519–1537. https://doi.org/10.5194/amt-10-1519-2017.
Skrifvars, B.-J., Backman, R., Hupa, M., Salmenoja, K., Vakkilainen, E., 2008. Corrosion of superheater steel materials under alkali salt deposits part 1: the effect of salt deposit composition and temperature. Corrosion Sci. 50, 1274–1282. https://doi.org/10.1016/j.corsci.2008.01.010.
Sorvajärvi, T., DeMartini, N., Rossi, J., Toivonen, J., 2014. In situ measurement technique for simultaneous detection of K, KCl, and KOH vapours released during combustion of solid biomass fuel in a single particle reactor. Appl. Spectrosc. 68, 179–184.
Stockwell, C.E., Christian, T.J., Goetz, J.D., Jayarathne, T., Bhave, P.V., Praveen, P.S., Adhikari, S., Maharjan, R., DeCarlo, P.F., Stone, E.A., Saikawa, E., Blake, D.R., Simpson, I.J., Yokelson, R.J., Panday, A.K., 2016. Nepal Ambient Monitoring and Source Testing Experiment (NAMaSTE): emissions of trace gases and light-absorbing carbon from wood and dung cooking fires,garbage and crop residue burning, brick kilns, and other sources. Atmos. Chem. Phys. 16, 11043–11081. https://doi.org/10.5194/acp-16-11043-2016.
Timonen, H., Karjalainen, P., Saukko, E., Saarikoski, S., Aakko-Saksa, P., Simonen, P., Murtonen, T., Dal Maso, M., Kuuluvainen, H., Bloss, M., Ahlberg, E., Svenningsson, B., Pagels, J., Brune, W.H., Keskinen, J., Worsnop, D.R., Hillamo, R., Rönkkö, T., 2017. Influence of fuel ethanol content on primary emissions and secondary aerosol formation potential for a modern flex-fuel gasoline vehicle. Atmos. Chem. Phys. 17, 5311–5329. https://doi.org/10.5194/acp-17-5311-2017.
Timonen, H., Karjalainen, P., Aalto, P., Saarikoski, S., Mylläri, F., Karvosenoja, N., Jalava, P., Asmi, E., Aakko-Saksa, P., Saukkonen, N., Laine, T., Saarnio, K., Niemela, N., Enroth, J., Vakeva, M., Oyola, P., Pagels, J., Ntziachristos, L., Cordero, R., Kuittinen, N., Niemi, J.V., Rönkkö, T., 2019. Adaptation of black carbon Footprint concept would accelerate mitigation of global warming. Environ. Sci. Technol. https://doi.org/10.1021/acs.est.9b05586.
Tissari, J., Lyyränen, J., Hytönen, K., Sippula, O., Tapper, U., Frey, A., Saarnio, K., Pennanen, A.S., Hillamo, R., Salonen, R.O., Hirvonen, M.R., Jokiniemi, J., 2008. Fine particle and gaseous emissions from normal and smouldering wood combustion in a conventional masonry heater. Atmos. Environ. 42, 7862–7873. https://doi.org/10.1016/j.atmosenv.2008.07.019.
Tiwari, M., Sahu, S.K., Bhangare, R.C., Yousaf, A., Pandit, G.G., 2014. Particle size distributions of ultrafine combustion aerosols generated from household fuels. Atmos. Pollut. Res. 5, 145–150.
Uski, O., Jalava, P.I., Happo, M.S., Torvela, T., Leskinen, J., Mäki-Paakkanen, J., Tissari, J., Sippula, O., Lamberg, H., Jokiniemi, J., Hirvonen, M.-R., 2015. Effect of fuel zinc content on toxicological responses of particulate matter from pellet combustion in vitro. Sci. Total Environ. 511, 331–340.
Wagner, J.P., Caraballo, S.A., 1997. Toxic species emissions from controlled combustion of selected rubber and plastic consumer products. Polym. Plast. Technol. Eng. 36, 189–224. https://doi.org/10.1080/03602559708000614.
Wiedinmyer, C., Yokelson, R.J., Gullett, B.K., 2014. Global emissions of trace gases, particulate matter, and hazardous air pollutants from open burning of domestic waste. Environ. Sci. Technol. 48, 9523–9530. https://doi.org/10.1021/es502250z.
Yli-Ojanperä, J., Kannosto, J., Marjamäki, M., Keskinen, J., 2010. Improving the nanoparticle resolution of the ELPI. Aerosol Air Qual. Res. 10, 360–366. https://doi.org/10.4209/aaqr.2009.10.0060.